Journal of Computational Mathematics, Vol.17, No.5, 1999, 463–474.

SPIRALS IN 2-D GAS DYNAMICS SYSTEMS*[1)]

Xiu-chuan Gu
(*Department of Mathematics, Jiamusi University, Jiamusi 154000, China*)

Shu-li Yang
(*Institute of Applied Mathematics, Academia Sinica, Beijing 100080, China*)

Li-xin Tao
(*Department of Computer Science, University of Concordia, Canada*)

Abstract

In this paper, the phenomena of spirals are numerically presented by MmB scheme [1] for initial value problems of 2-D gas dynamics ($\gamma = 1.4$), which include 2-D Riemann problems and continuous initial value problems. The numerical results are well coincide with on the exact solution in [2] and the conjectures on solution structure in [3] for 2-D isentropic and adiabatic flows. In isentropic flow, for high speed rotation ($v_0/c_0 > \sqrt{2}$), there is a region of vacuum at the origin and for low speed rotation ($v_0/c_0 < \sqrt{2}$), there is no vacuum, and for adiabatic flow, the structure of spirals is also discussed.

Key words: Spiral, MmB scheme, Conservation laws.

1. Preliminaries

(I) Models

Consider the two models: isentropic and adiabatic flows,

(a) 2-D isentropic flow

$$\begin{cases} \rho_t + (\rho u)_x + (\rho v)_y = 0 \\ (\rho u)_t + (\rho u^2 + p)_x + (\rho uv)_y = 0 \\ (\rho v)_t + (\rho uv)_x + (\rho v^2 + p)_y = 0 \end{cases} \tag{1.1}$$

(b) 2-D adiabatic flow

$$\begin{cases} \rho_t + (\rho u)_x + (\rho v)_y = 0 \\ (\rho u)_t + (\rho u^2 + p)_x + (\rho uv)_y = 0 \\ (\rho v)_t + (\rho uv)_x + (\rho v^2 + p)_y = 0 \\ (\rho(e + \frac{u^2+v^2}{2}))_t + (\rho u(h + \frac{u^2+v^2}{2}))_x + (\rho v(h + \frac{u^2+v^2}{2}))_y = 0 \end{cases} \tag{1.2}$$

* Received June 6, 1995.
[1)] Supported by NNSF of China.

$$e = \frac{p}{(\gamma - 1)\rho}, \qquad h = e + \frac{p}{\rho}$$

where ρ, (u,v) and p is density, velocity and presure, respectively.
and with the 2-D Riemann data

$$(\rho, u, v)|_{t=0} = (\rho_i, u_i, v_i), \quad (i) = 1, 2, 3, 4 \tag{1.3}$$

or

$$(\rho, p, u, v)|_{t=0} = (\rho_i, p_i, u_i, v_i), \quad (i) = 1, 2, 3, 4 \tag{1.4}$$

where (i)-states are described to

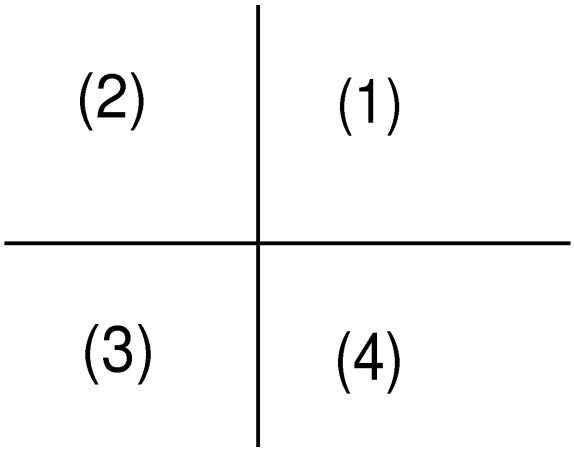

Problem (1.1)(1.3) and (1.2) (1.4) have theoretically studied by characteristic methods [2], and a set of conjectures on the solution structure were presented for the 2-D Riemann problem under the assumption,

Assumption: Each jump in initial data outside the origin projectes exactly one shock wave, rarefaction wave, and slip planes.

The most most interesting conjecture is that there is a spiral in the solution for some Riemann data.

The exact solutions were obtained in the case $\gamma = 2$ for isentropic flow by Zhang and Zheng in [2], the initial data were taken to

$$(u, v, \rho)|_{t=0} = (v_0 \sin\theta, -v_0 \cos\theta, \rho_0)$$

and they got the conclusion that for **high speed rotation** $2c_0^2 < v_0^2$ ($c_0 = \sqrt{p_\rho}$), the solution has region of vacuum at the center; for **low speed rotation** $2c_0^2 > v_0^2$, the solution has no vacuum.

(II) Characteristics and choices of initial data

The system (1.1) and (1.2), for smooth solutions, can be written to,

$$\begin{pmatrix} \rho \\ u \\ v \end{pmatrix}_t + \begin{pmatrix} u & \rho & 0 \\ p'/\rho & u & 0 \\ 0 & 0 & u \end{pmatrix} \begin{pmatrix} \rho \\ u \\ v \end{pmatrix}_x + \begin{pmatrix} v & 0 & \rho \\ 0 & v & 0 \\ p'/\rho & 0 & v \end{pmatrix} \begin{pmatrix} \rho \\ u \\ v \end{pmatrix}_y = 0 \tag{1.5}$$

and

$$\begin{pmatrix} \rho \\ u \\ v \\ p \end{pmatrix}_t + \begin{pmatrix} u & \rho & 0 & 0 \\ 0 & u & 0 & 1/\rho \\ 0 & 0 & u & 0 \\ 0 & \gamma p & 0 & u \end{pmatrix} \begin{pmatrix} \rho \\ u \\ v \\ p \end{pmatrix}_x + \begin{pmatrix} v & 0 & \rho & 0 \\ 0 & v & 0 & 0 \\ 0 & 0 & v & 1/\rho \\ 0 & 0 & \gamma p & v \end{pmatrix} \begin{pmatrix} \rho \\ u \\ v \\ p \end{pmatrix}_y = 0 \tag{1.6}$$

then the characteristic roots are

$$\lambda_0 = u, \quad \lambda_\pm = u \pm c$$

where c is sound speed $c = \sqrt{p'}$ for isentropic flow and $c = \sqrt{\gamma p/\rho}$ for adiabatic flow. From [2], we list the following conditions to choose initial data that satisfy the assumption in the above section.

(i) conditions for rarefaction waves.

$$v_1 = v_2, \quad u_2 = u_1 \pm \int_{\rho_1}^{\rho_2} \frac{\sqrt{p'}}{\rho} d\rho, \quad \text{for isentropic flow}$$

or

$$v_1 = v_2, \quad u_2 = u_1 \pm \int_{\rho_1}^{\rho_2} \frac{c}{\rho} d\rho, \quad d(p\rho^{-\gamma}) = 0, \quad \text{for adiabatic flow}$$

where $\pm$ is relate to forward rarefaction wave ($\overrightarrow{R}$) or backward rarefaction wave ($\overleftarrow{R}$).

(ii) conditions for shock waves.

$$v_2 = v_1, \quad u_2 = u_1 \pm \left(\sqrt{\frac{\rho_2}{\rho_1} p'_{12}} - \sqrt{\frac{\rho_1}{\rho_2} p'_{21}}\right), \ \rho_2 > \rho_1 \text{ or } \rho_2 < \rho_1, \ \text{for isentropic flow}$$

or

$$v_2 = v_1, \quad u_2 = u_1 \pm \left(\sqrt{\frac{\rho_2}{\rho_1} p'_{12}} - \sqrt{\frac{\rho_1}{\rho_2} p'_{21}}\right), \quad \frac{p_2}{p_1} = \frac{(\gamma+1)\rho_2 - (\gamma-1)\rho_1}{(\gamma+1)\rho_1 + (\gamma-1)\rho_2},$$
$$\rho_2 > \rho_1 \text{ or } \rho_2 < \rho_1, \quad \text{for adiabatic flow}$$

where $p'_{12} = p'_{21} = \frac{p_2 - p_1}{\rho_2 - \rho_1}$, $\pm$ is forward shock wave ($\overrightarrow{S}$) or backward shock wave ($\overleftarrow{S}$).

(iii) conditions for contact discontinuities.

$$u_2 = u_1, \quad \rho_2 = \rho_1, \quad \text{for isentropic flow}$$

or

$$u_2 = u_1, \quad p_2 = p_1, \quad \text{for adiabatic flow}$$

then the direction of a contact discontinuity was defined as

$$J^{\pm} := Curl(u,v) = v_x - u_y = \pm\infty$$

There are two kinds of distributions for velocity (u,v) according to the signals of J's. If the four Js have same signals, the distribution of velocity is in a counter clockwise direction; if not same, the distribution of velocity is in a clockwise direction. See Figure 1.1.

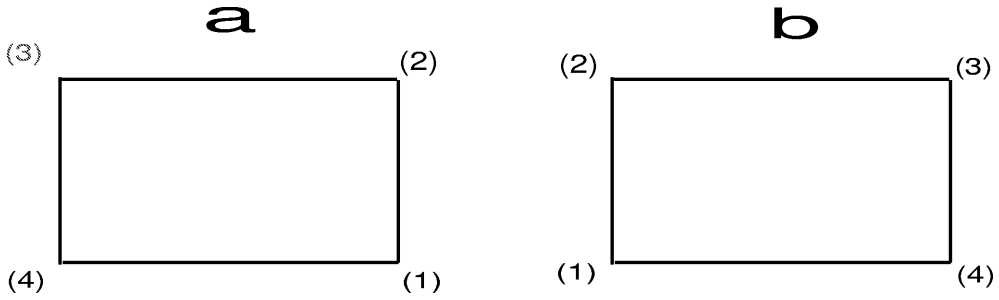

Figure 1.1: a. counter clockwise, b. clockwise

For the different distribution of the velocity, there are two kinds of great different solutions. For the same signal of Js, there is spiral in the solution [3]; otherwise there are shock waves or more singular waves in the solutions (see [4]).

(III) Numerical method

The numerical solutions are presented by using MmB (locally Maximum-minimum Bounds preserving) schemes, which have high resolution and nonoscillatory properties. For 2-D scalar conservation law, the solution of the scheme ($u_{i,j}^{n+1} = (Lu^n)_{i,j}$) satisfys:

$u_{i,j}^{n+1}$ is a convex combination of the point values at step n

The generalized of MmB scheme form is for the following 2-D hyperbolic systems $U_t + F(U)_x + G(U)_y = 0$,

$$
\begin{aligned}
&U_{i,j}^{n+1} = U_{i,j}^n \\
&-A^+_{i-\frac{1}{2},j}\lambda_x\Delta_x u^n_{i-\frac{1}{2},j} - \tfrac{1}{2}\lambda_x\Delta_{-,x}(T^x_{i+\frac{1}{2},j}\Lambda^{x,}_{i+\frac{1}{2},j}(I-\Lambda^{x,+}_{i+\frac{1}{2},j}\lambda_x)S^{x,-}_{i+\frac{1}{2},j}T^{x,-1}_{i+\frac{1}{2},j}\Delta_x U^n_{i+\frac{1}{2},j}) \\
&-A^-_{i+\frac{1}{2},j}\lambda_x\Delta_x U^n_{i+\frac{1}{2},j} + \tfrac{1}{2}\lambda_x\Delta_{-,x}(T^x_{i+\frac{1}{2},j}\Lambda^{x,-}_{i+\frac{1}{2},j}(I+\Lambda^{x,-}_{i+\frac{1}{2},j}\lambda_x)S^{x,+}_{i+\frac{1}{2},j}T^{x,-1}_{i+\frac{1}{2},j}\Delta_x U^n_{i+\frac{1}{2},j}) \\
&-B^+_{i-\frac{1}{2},j}\lambda_y\Delta_y U^n_{i,j-\frac{1}{2}} - \tfrac{1}{2}\lambda_y\Delta_{-,y}(T^y_{i,j+\frac{1}{2}}\Lambda^{y,+}_{i,j+\frac{1}{2}}(I-\Lambda^{y,+}_{i,j+\frac{1}{2}}\lambda_y)S^{y,-}_{i,j+\frac{1}{2}}T^{y,-1}_{i,j+\frac{1}{2}}\Delta_y U^n_{i,j+\frac{1}{2}}) \\
&-B^-_{i,j+\frac{1}{2}}\lambda_y\Delta_y U^n_{i,j+\frac{1}{2}} + \tfrac{1}{2}\lambda_y\Delta_{-,y}(T^y_{i,j+\frac{1}{2}}\Lambda^{y,-}_{i,j+\frac{1}{2}}(I+\Lambda^{y,-}_{i,j+\frac{1}{2}}\lambda_y)S^{y,+}_{i,j+\frac{1}{2}}T^{y,-1}_{i,j+\frac{1}{2}}\Delta_y U^n_{i,j+\frac{1}{2}}) \\
&+\tfrac{1}{2}\lambda_x\lambda_y[A^+_{i-\frac{1}{2},j-\frac{1}{2}}\Delta_x(B^+_{i-\frac{1}{2},j-\frac{1}{2}}\Delta_y U^n_{i-\frac{1}{2},j-\frac{1}{2}}) + B^+_{i-\frac{1}{2},j-\frac{1}{2}}\Delta_y(A^+_{i-\frac{1}{2},j-\frac{1}{2}}\Delta_x U^n_{i-\frac{1}{2},j-\frac{1}{2}})] \\
&-\tfrac{1}{2}\lambda_x\lambda_y[A^+_{i-\frac{1}{2},j+\frac{1}{2}}\Delta_x(B^-_{i-\frac{1}{2},j+\frac{1}{2}}\Delta_y U^n_{i-\frac{1}{2},j+\frac{1}{2}}) + B^-_{i-\frac{1}{2},j+\frac{1}{2}}\Delta_y(A^+_{i-\frac{1}{2},j+\frac{1}{2}}\Delta_x U^n_{i-\frac{1}{2},j+\frac{1}{2}})] \\
&-\tfrac{1}{2}\lambda_x\lambda_y[A^-_{i+\frac{1}{2},j-\frac{1}{2}}\Delta_x(B^+_{i+\frac{1}{2},j-\frac{1}{2}}\Delta_y U^n_{i+\frac{1}{2},j-\frac{1}{2}}) + B^+_{i+\frac{1}{2},j-\frac{1}{2}}\Delta_y(A^-_{i+\frac{1}{2},j-\frac{1}{2}}\Delta_x U^n_{i+\frac{1}{2},j-\frac{1}{2}})] \\
&+\tfrac{1}{2}\lambda_x\lambda_y[A^-_{i+\frac{1}{2},j+\frac{1}{2}}\Delta_x(B^-_{i+\frac{1}{2},j+\frac{1}{2}}\Delta_y U^n_{i+\frac{1}{2},j+\frac{1}{2}}) + B^-_{i+\frac{1}{2},j+\frac{1}{2}}\Delta_y(A^-_{i+\frac{1}{2},j+\frac{1}{2}}\Delta_x U^n_{i+\frac{1}{2},j+\frac{1}{2}})]
\end{aligned}
$$

where

$$\Phi_{ij}^{x(y)} = T^{x(y)}(\Phi_{ij}^{diag,x(y),+} + \Phi_{ij}^{diag,x(y),-})T^{x(y),-1}$$
$$\partial F = A(U)\partial U \qquad \partial G = B(U)\partial U$$
$$A(U) = T^x \Lambda^x T^{x,-1}, \qquad \Lambda^x = diag(\mu_1^x, \mu_2^x, ..., \mu_n^y)$$
$$B(U) = T^x \Lambda^y T^{y,-1}, \qquad \Lambda^y = diag(\mu_1^y, \mu_2^y, ..., \mu_n^y)$$
$$\Phi_{ij}^{diag,x(y),\pm} = diag(\Phi_{ij}^{x(y),\mu_1^{x(y)},\pm}, ..., \Phi_{ij}^{x(y),\mu_n^{x(y)},\pm})$$
$$\Phi_i^{x(y),\mu_k^{x(y)},\pm} = \int_x^{x(y)+\mu_k^{x(y),\pm}\Delta t} \overline{\phi}_{ij} dx$$
$$\mu_k^{x(y),\pm} = \frac{1}{2}(\mu_k^{x(y)} \pm |\mu_k^{x(y)}|), \quad k = 1, 2, ..., n$$

$$S_{i+\frac{1}{2},j}^{x,\pm} = diag(s_{i+\frac{1}{2},j}^{1,x,\pm}, ..., s_{i+\frac{1}{2}}^{n,x,\pm}, j)$$
$$S_{i,j+\frac{1}{2}}^{y,\pm} = diag(s_{i,j+\frac{1}{2}}^{1,y,\pm}, ..., s_{i,j+\frac{1}{2}}^{n,y,\pm})$$

$$s_{i+\frac{1}{2},j}^{k,x,+} = \frac{(T_{i-\frac{1}{2},j}^{x,-1}\Delta_x U_{i-\frac{1}{2}}^n, j)^k}{(T_{i+\frac{1}{2},j}^{x,-1}\Delta_x U_{i+\frac{1}{2}}^n, j)} \qquad s_{i+\frac{1}{2},j}^{k,x,-} = \frac{(T_{i+\frac{3}{2},j}^{x,-1}(\Delta_x U_{i+\frac{3}{2},j}^n)^k}{(T_{i+\frac{1}{2},j}^{x,-1}\Delta_x U_{i+\frac{1}{2},j}^n)^k}$$

$$s_{i,j+\frac{1}{2}}^{k,y,+} = \frac{(T_{i,j-\frac{1}{2}}^{y,-1}\Delta_y U_{i,j-\frac{1}{2}}^n)^k}{(T_{i,j+\frac{1}{2}}^{y,-1}\Delta_y U_{i,j+\frac{1}{2}}^n)} \qquad s_{i,j+\frac{1}{2}}^{k,y,-} = \frac{(T_{i,j+\frac{3}{2}}^{y,-1}(\Delta_y U_{i,j+\frac{3}{2}}^n)^k}{(T_{i,j+\frac{1}{2}}^{y,-1}\Delta_y U_{i,j+\frac{1}{2}}^n)^k}$$

$$k = 1,\ 2,\ ...,\ n$$

In this paper, we only consider the case that contact discontinuities have same signal in initial data, that is, the velocity of initial data is in the counter clockwise distribution. In section 2 and 3, spirals, which contain the two cases, low speed rotation and high speed rotation, are numerical presented by MmB schemes for isentropic flow and adiabatic flow, respectively.

2. Isentropic Flow

For the model of isentropic flow, the exact solution has been obtained by Zhang and Zheng [3] for $\gamma = 2$, then they studied the solution structure for the initial data,

$$(\rho_0, u_0, v_0) = (v_0 \sin\theta, v_0 \cos\theta, \rho_0) \tag{2.1}$$

where θ belongs to the polar coordinates (r, θ)

$$x = r\cos\theta, \quad y = r\sin\theta$$

They defined:

$$2p'(\rho_0) < v_0^2, \qquad \text{high speed rotation}$$

$$2p'(\rho_0) > v_0^2, \qquad \text{low speed rotation}$$

and got the conclusion: the solution of density has region of vacuum at the center for high speed rotation and no vacuum for low speed rotation. Here we present the numerical solutions for both continuous initial data (2.1) and 2-D Riemann problems in the case ($\gamma = 1.4$). The distributions of velocity are described as,

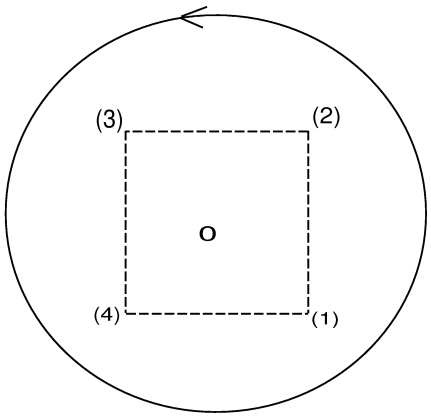

It is counter clockwise related to four constants.

As defined in [3], here we divid initial data into two classes: low speed rotation and high speed rotation.

(I) low speed rotation.

The continuous data are choosen to:

$$v_0 = 1, \quad \rho_0 = 20$$

See Figure 2.1,

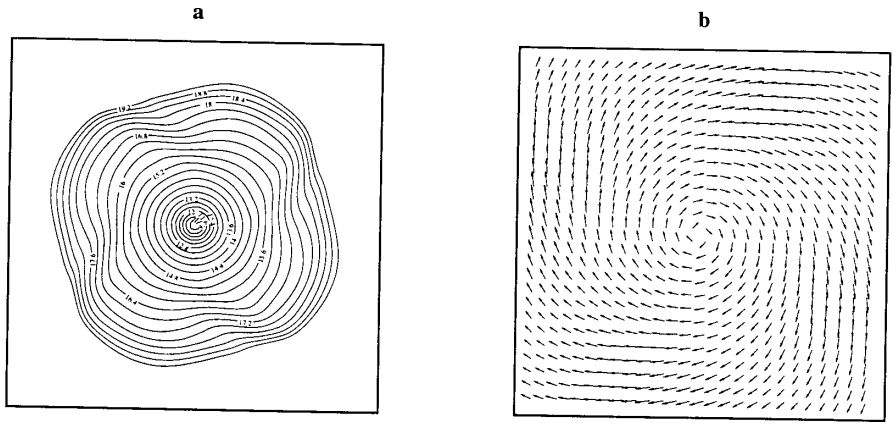

Figure 2.1: a. Density contour lines b. Velocity field
n=200 M-P=101 $\times$ 101 $\lambda = 0.08$

For Riemann data

$$u_1 = u_2 = -u_3 = -u_4 = 1, \quad v_2 = -v_1 = v_3 = -v_4 = 1,$$

$$\rho_1 = \rho_2 = \rho_3 = \rho_4 = 20$$

See Figure 2.2

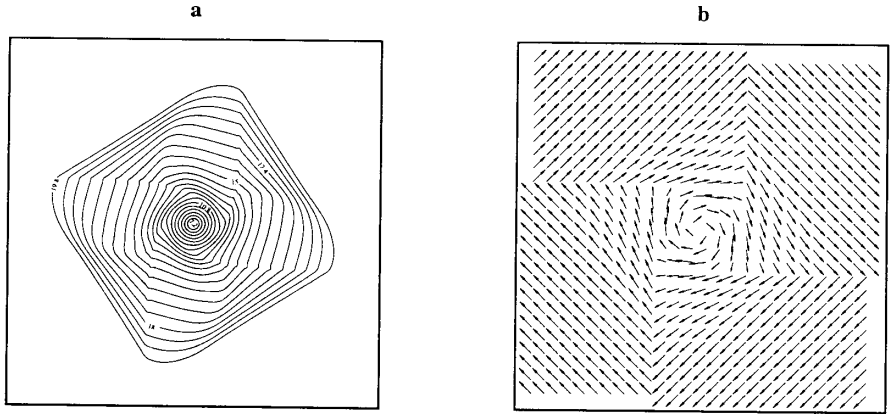

Figure 2.2: a. Density Contour Lines b. Velocity Field
n=250 M-P=201 $\times$ 201, $\lambda = 0.1$

Here and in the following, n and M-P expresses time steps and mesh points, respectively. From the velocity fields of Figures (2.1) and (2.2), we know that there is a spiral in each case, and from labels for the density contour lines, there is no vacuum in the low speed rotation, in the case $v_o/c_o < \sqrt{2}$, here choose $v_o = \max_i \sqrt{u_i^2 + v_i^2}$ for Riemann problem.

(II) high speed rotation

For continuous data,

$$v_0 = 3, \quad \rho_0 = 1$$

See Figure 2.3,

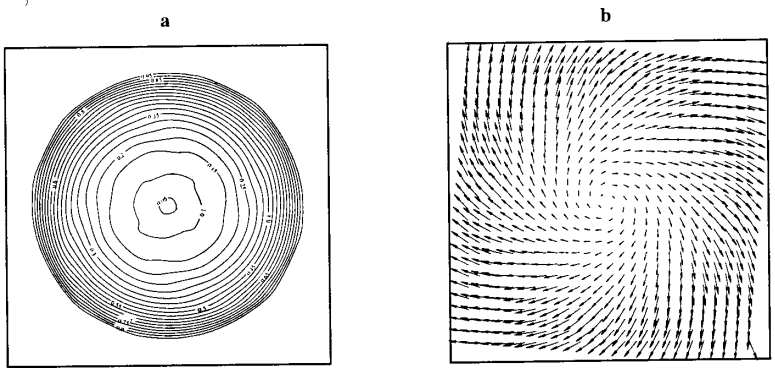

Figure 2.3: a. Density contour lines b. Velocity field
n=200 M-P=101 $\times$ 101 $\lambda = 0.08$

for Riemann data

$$u_1 = u_2 = -u_3 = -u_4 = 3, \quad v_2 = -v_1 = v_3 = -v_4 = 3,$$

$$\rho_1 = \rho_2 = \rho_3 = \rho_4 = 1$$

See Figure 2.4

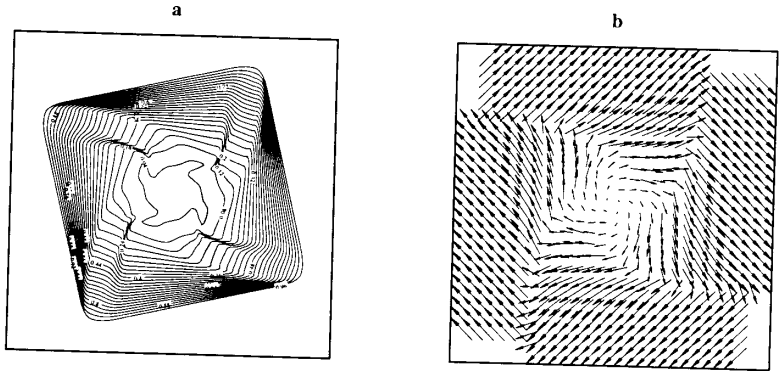

Figure 2.4: a. Density contour lines b. Velocity field
n=200 M-P=151 $\times$ 151, $\lambda = 0.1$

From the density contour lines in Figures 2.3 and 2.4, we can see that the density is zero in the region of the center (0,0). In the region, the velocity is almost to zero, and the region of vacuum is serround by a rotation. The results are well coincide with the conclusion of paper [3].

3. Adiabatic Flow

For adiabatic flow, as we known, there is no exact solution even for special initial value problem. In [3], the conjecture on the spiral was presented for only containing four contact discontinuities on initial data. In this section, we present two classes of numerical solutions for both continuous initial data and Riemann data to justify solution structure and compare to the solution structure for isentropic flow.

Here we list the numerical results by density, pressure and pseudo-Mach number contour lines, and velocity fields in the figures, where pseudo-Mach number is written to,

$$V/c, \quad V = (u - x/t, v - y/t)$$

(i) the solutions no vacuum region.
For continuous initial data, we take:

$$u_o = \sin\theta, \quad v_o = -\cos\theta, \quad \rho_0 = 0.5 + |\sin\theta|, \quad p_o = 20.$$

See Figure 3.1,

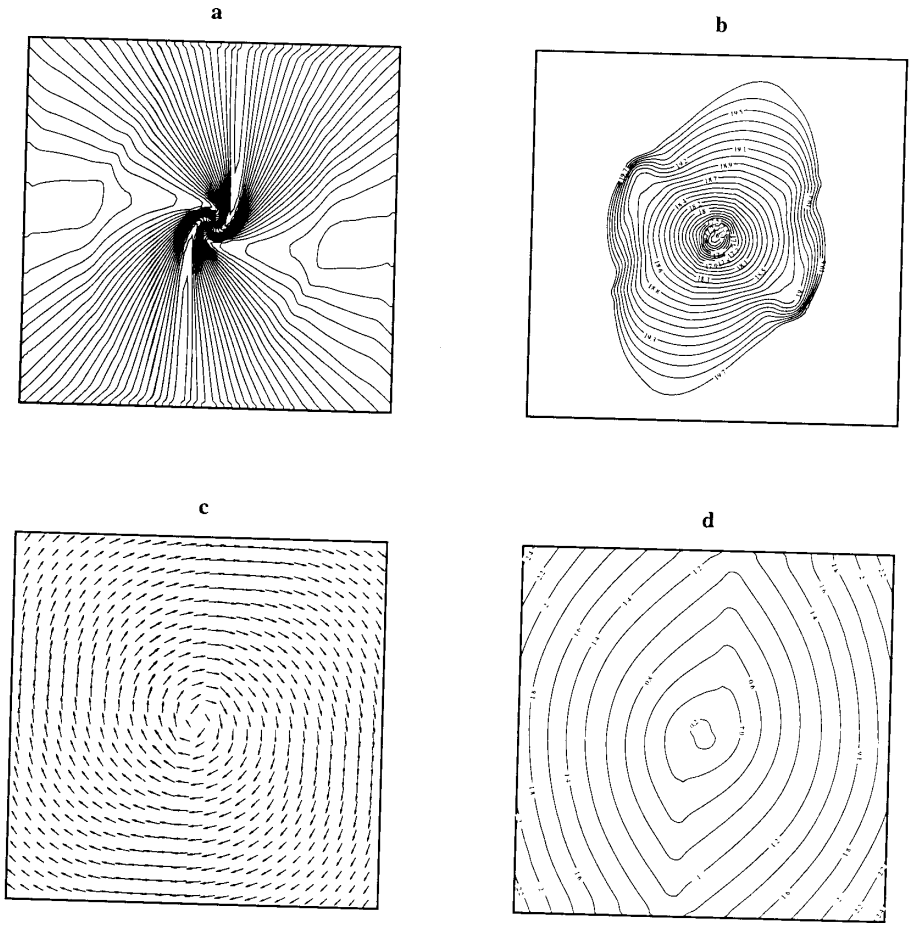

Figure 3.1: a. Density contour lines b. Pressure contour lines
c. Velocity Field d. Pseudo-Mach contour lines
n=120 M-P=101 $\times$ 101, $\lambda = 0.08$

For 2-D Riemann data: (see Figure 3.2)

$$u_1 = u_2 = -u_3 = -u_4 = 1.0, \quad v_1 = -v_2 = -v_3 = v_4 = -1.0$$

$$\rho_1 = \rho_3 = 1.5, \quad \rho_2 = \rho_4 = 0.5, \quad p_1 = p_2 = p_3 = p_4 = 20.$$

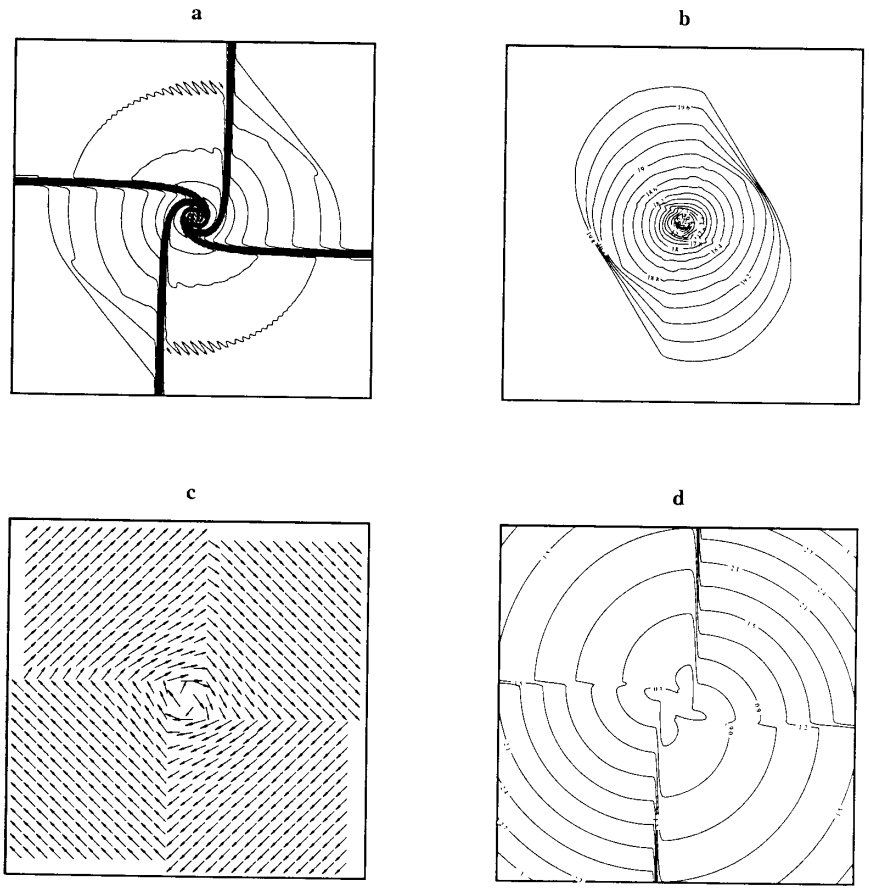

Figure 3.2: a. Density contour lines b. Pressure contour lines
c. Velocity field d. Pseudo-Mach contour lines
n=200 M-P=201 $\times$ 201, $\lambda = 0.08$

(i) the solutions containing vacuum region.

For continuous initial data: (see Figure 3.3)

$$u_o = 2\sin\theta, \quad v_o = -2\cos\theta, \quad \rho_0 = 0.5 + |\sin\theta|, \quad p_o = 2.$$

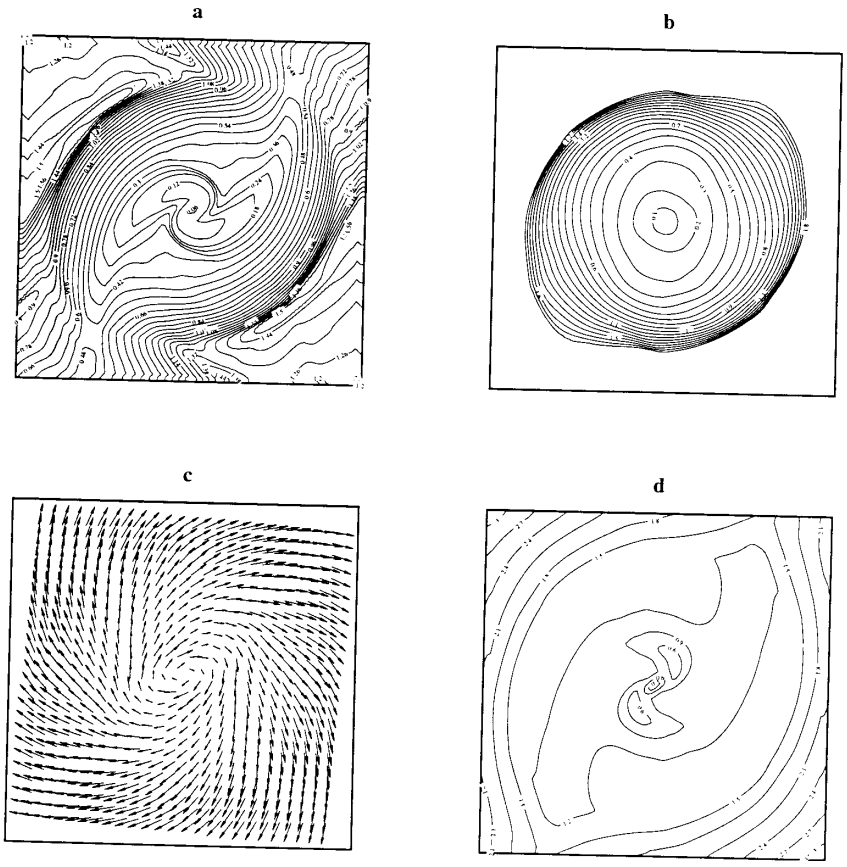

Figure 3.3: a. Density contour lines b. pressure contour lines
c. Velocity field d. Pseudo-Mach contour lines
n=160 M-P=101 $\times$ 101, $\lambda = 0.1$

For 2-D Riemann data: (see Figure 3.4)

$$u_1 = u_2 = -u_3 = -u_4 = 2.0, \quad v_1 = -v_2 = -v_3 = v_4 = -2.0$$

$$\rho_1 = \rho_3 = 1.5, \quad \rho_2 = \rho_4 = 0.5, \quad p_1 = p_2 = p_3 = p_4 = 2.$$

In Figures 3.1 and 3.2, the density of the solutions has no vacuum region for the low speed rotation, and Figures 3.3 and 3.4, there are vacuum regions in the solutions of the density. However the initial data do not satisfy the condition given in [2] when the solutions have vacuum states from Figures 3.3 and 3.4. By pseudo-Mach number contour lines, we clearly see the subsonic, transonic and supersonic regions in pseudo-stationary.

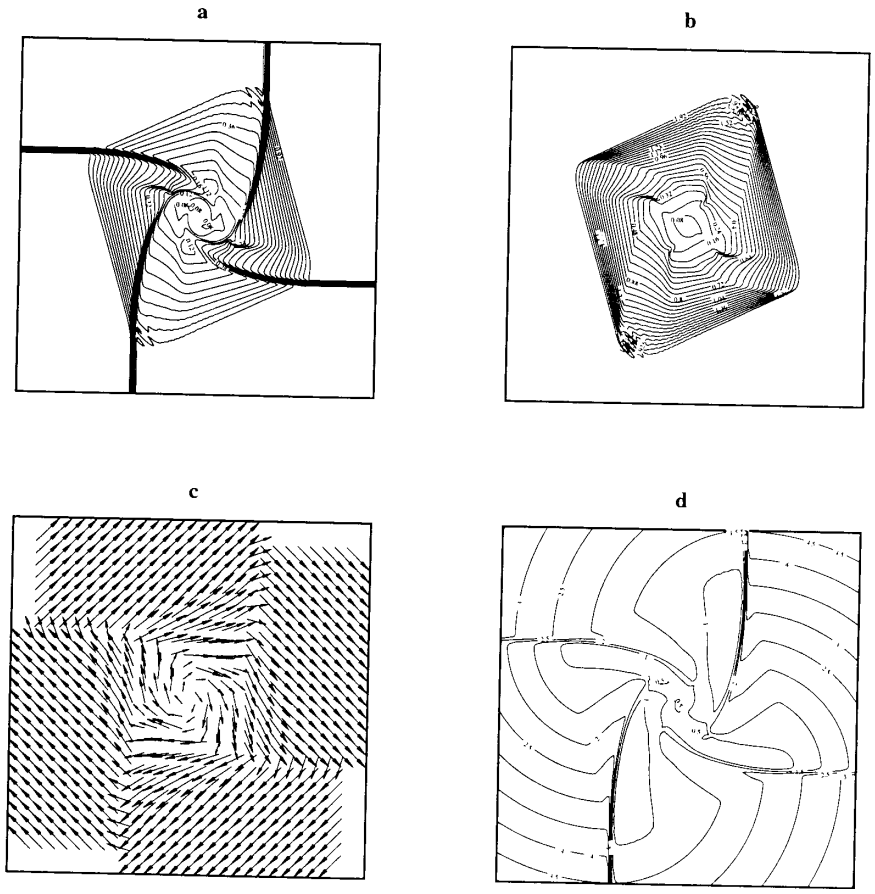

Figure 3.4: a. Density contour lines b. Pressure contour lines
c. Velocity field d. Pseudo-Mach contour lines
n=200 M-P=151 $\times$ 151, $\lambda = 0.1$

References

[1] S.L. Yang, T. Zhang, The MmB difference solutions of Riemann problems for two dimensional 2×2 nonlinear conservation laws, *IMPACT of Computing in Science and Engineering,* **3** (1991), 146-180.

[2] T. Zhang, Y.X. Zheng, Conjecture on the structure of solutions of the Riemann problem for two-dimensional gas dynamics systems, *SIAM J. Math. Anal.,* **21** (1990), 593-630.

[3] T. Zhang, Y.X. Zheng, Exact spiral solutions of the two dimensional compressible Euler equations, to appear.

[4] S.L. Yang, Lixin Tao, Singularities in solutions for 2-D gas dynamics systems, in preparation.